

On the influence of the "short- and open-circuit" conditions on stability loss of the PZT/Metal/PZT sandwich circular plate-disc condition

Fazile I. Jafarova

Received: 12.03.2017 / Revised: 05.07.2017 / Accepted: 21.10.2017

Abstract. *The axisymmetric stability loss of the PZT/Metal/PZT sandwich circular plate is investigated simultaneously within the scope of the open-circuit and short-circuit electrical conditions. It is assumed that these conditions satisfy on the upper and lower face-planes of the piezoelectric layers. Moreover, it is assumed that on the lateral-boundary cylindrical surfaces of the piezoelectric face layers the short-circuit conditions satisfy. The 3D linearized stability loss theory for piezoelectric materials is employed for investigation of the corresponding eigenvalue problem. Concrete numerical results are obtained by utilizing FEM for various piezoelectric face and metal core layers and the main attention is focused on the influence of the piezoelectricity on the values of the compressional critical stress and the influence of the aforementioned two type electrical boundary conditions on these stresses. According to the comparison of the results, it is made conclusions on the significance of the influence of the electrical boundary conditions on the values of the absolute values of the critical stresses. In particular, it is established that in the case where the open-circuit boundary conditions satisfy the influence of the piezoelectricity of the face layers materials on the critical stresses is more significant than that in the case where the short-circuit boundary conditions satisfy.*

Keywords. Piezoelectric material · open-circuit, short-circuit · circular sandwich plate · stability loss · critical stress

Mathematics Subject Classification (2010): 74H55

1 Introduction

Investigations of stability loss of plate type element of constructions made of piezoelectric materials (shortly PZT) or made of layered composites containing PZT layers has a great significance not only in the theoretical, but also in the practical sense. Researchers such as [11], Jerom and Ganesan (2010) and many others listed therein can be taken as examples

for such investigations in which it was established that the piezoelectricity of the plate or beam materials causes an increase in the values of the mechanical critical forces

Now we consider a brief review of the related recent investigations and first note the paper by [10] in which static analysis of the simply supported rectangular plate made of functionally graded piezoelectric material is studied with the use of the refined plate theories. The “open- and closed- circuit” conditions on the upper and lower face surfaces are considered. The paper by [4] deals with the study the response of the bi-layered circular plate made of functionally-graded piezoelectric material and resting on a Winkler-Pasternak foundation.

[7] studies the buckling of the sandwich circular plate with piezoelectric face and porous middle layers under radial compression within the scope of the Kirchhoff-Love plate theory and therefore results obtained in this paper are acceptable for very thin plates. The analytical expression for the critical force is obtained and according to this expression the influence of the problem parameters, as well as of the piezoelectricity of the covering layer material is discussed.

The foregoing brief review shows that all the foregoing investigations have been made within the scope of the approximate plate theories, the accuracy of which depends significantly on the geometrical and electro-mechanical properties. It is obvious that the order of the accuracy of these results can be estimated with the use of the corresponding results obtained within the scope of the 3D linearized exact stability loss theories the present level of which has been detailed in the monograph by [5] who made many fundamental contributions to creating this theory. At the same time we note that the 3D linearized stability loss theories for the elements of constructions made of time-dependent materials was developed in the monograph by [1].

In the foregoing sense, in the paper by [2] the first attempt with respect to the stability loss problems related to the system comprising elastic and piezoelectric constituents was made. At the same time, it should be noted that the study of stability loss of elements of constructions made of piezoelectric materials by employing 3D linearized stability loss theories just is beginning.

One of the main question in the theory of piezoelectricity, as well as in the investigations of a stability loss of element of constructions made of these materials, is the study the influence of the “open-circuit” and “short-circuit” type electrical boundary conditions on the electro-mechanical behavior of these constructions. Taking the this statement into consideration in the present paper the aforementioned influence is studied for the circular sandwich PZT/Metal/PZT plate within the scope of the 3D linearized stability loss theory. Under this study it is assumed that the plate is compressed in the radial inward direction by uniformly distributed rotationally symmetric normal forces.

We recall that the corresponding 3D stability loss problems for the circular plate consisting of elastic and viscoelastic constituents are made in the papers by [3] and [9] the results of which are also detailed in the monograph by [1].

2 Formulation of the problem

We consider a circular sandwich plate whose geometry is shown in Fig. 1 and assume that the materials of the upper and lower face layer are the same and PZT.

We associate with the lower face layer of the plate the cylindrical coordinate system $Or\theta z$ (Fig. 1) and the position of the points of the plate we determine through the Lagrange coordinates in this system. Thus, according to Fig.1, in the selected coordinate system, the plate occupies the region $\{0 \leq r \leq \ell/2; 0 \leq \theta \leq 2\pi; 0 \leq z \leq h\}$. Investigate the axisymmetric (rotationally symmetric) stability loss of the mentioned plate under compression of

that in the inward radial direction by uniformly distributed rotationally symmetric normal forces with intensity p acting on the lateral boundary-surface.

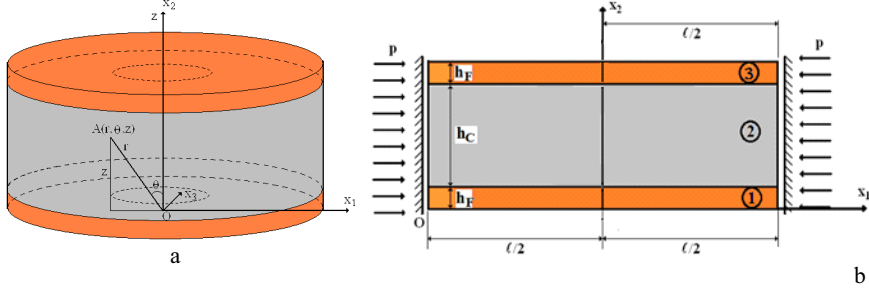


Fig. 1. The geometry of the considered circular plate (a) and the cross section of this plate with loading condition and some geometric values (b).

Below we will denote the values related to the upper and lower face layers by upper indices (2.3) and (2.1) respectively, whereas the values related to the core layer are denoted by (2.2). Moreover, the values related to the pre-critical stress-strain state are denoted by additional upper index 0.

Under investigations we will consider two type boundary conditions on the upper and lower face planes of the PZT layers. The first type of these conditions are the “open-circuit” ones, according to which it is assumed that $D_z^1 = 0$ at $z = 0$ and h_F , and $D_z^3 = 0$ at $z = h_c + h_F$ and $h_c + 2h_F$, $D_z^{(k)}$ is a normal component of the electric displacement. The second type conditions are the “short-circuit” ones, according to which, $\phi^1 = 0$ at $z = 0$ and h_F , and $\phi^3 = 0$ at $z = h_c + h_F$ and $h_c + 2h_F$, where $\phi^{(k)}$ is a potential of an electric field and $E_r^{(k)} = -\partial\phi^{(k)}/\partial r$, $E_z^{(k)} = -\partial\phi^{(k)}/\partial z$. Here $E_r^{(k)}$ and $E_z^{(k)}$ are the radial and normal component of the electric field vector.

In the case where the “open-circuit” conditions take place the pre-critical stress state is determined according to the following expressions:

$$\begin{aligned} \sigma_{zz}^{(k),0} &= 0, \sigma_{rr}^{(k),0} = 0, s_{zz}^{(k),0} = 0, D_z^{(k),0} = D_r^{(k),0} = 0, k = 1, 2, 3. \\ E_r^{(k),0} &= a_1^{(k)} s_{rr}^{(k),0} + b_1^{(k)} s_{zz}^{(k),0}, E_z^{(k),0} = d_1^{(k)} s_{rr}^{(k),0} + c_1^{(k)} s_{zz}^{(k),0}, \\ a_1^{(k)} &= \frac{\varepsilon_{13}^{(k)} (e_{31}^{(k)} + e_{32}^{(k)}) - \varepsilon_{33}^{(k)} (e_{11}^{(k)} + e_{22}^{(k)})}{\varepsilon_{11}^{(k)} \varepsilon_{33}^{(k)} - \varepsilon_{13}^{(k)} \varepsilon_{31}^{(k)}}, b_1^{(k)} = \frac{\varepsilon_{13}^{(k)} e_{33}^{(k)} - \varepsilon_{33}^{(k)} e_{13}^{(k)}}{\varepsilon_{11}^{(k)} \varepsilon_{33}^{(k)} - \varepsilon_{13}^{(k)} \varepsilon_{31}^{(k)}}, \\ d_1^{(k)} &= \frac{\varepsilon_{11}^{(k)} (e_{31}^{(k)} + e_{32}^{(k)}) - \varepsilon_{31}^{(k)} (e_{11}^{(k)} + e_{12}^{(k)})}{\varepsilon_{13}^{(k)} \varepsilon_{31}^{(k)} - \varepsilon_{11}^{(k)} \varepsilon_{33}^{(k)}}, c_1^{(k)} = \frac{\varepsilon_{11}^{(k)} e_{33}^{(k)} - \varepsilon_{31}^{(k)} e_{13}^{(k)}}{\varepsilon_{13}^{(k)} \varepsilon_{31}^{(k)} - \varepsilon_{11}^{(k)} \varepsilon_{33}^{(k)}}. \\ s_{zz}^{(k),0} &= a_{zr}^{(k)} s_{rr}^{(k),0}, a_{zr}^{(k)} = \frac{c_{31}^{(k)} + c_{32}^{(k)} - e_{13}^{(k)} a_1^{(k)} - e_{33}^{(k)} d_1^{(k)}}{c_{33}^{(k)} - e_{13}^{(k)} b_1^{(k)} - e_{33}^{(k)} c_1^{(k)}}. \\ \sigma_{rr}^{(k),0} &= A_r^{(k)} s_{rr}^{(k),0}, A_r^{(k)} = c_{11}^{(k)} + c_{12}^{(k)} - e_{11}^{(k)} a_1^{(k)} + \\ &+ a_{zr}^{(k)} c_{13}^{(k)} - a_{zr}^{(k)} e_{11}^{(k)} b_1^{(k)} - a_{zr}^{(k)} e_{31}^{(k)} c_1^{(k)}. \end{aligned}$$

$$s_{rr}^{(1),0} = s_{rr}^{(2),0}, 2h_f \sigma_{rr}^{(1),0} + h_c \sigma_{rr}^{(2),0} = hp, \sigma_{rr}^{(1),0} = p \left(2 \frac{h_F}{h} + \frac{h_C}{h} \frac{A_r^{(2)}}{A_r^{(1)}} \right)^{-1}. \quad (2.1)$$

In (2.1) $\sigma_{rr}^{(k),0}, \dots$, and $s_{rr}^{(k),0}, \dots$, are the components of the stress and Green strain tensors, respectively, $u_r^{(k),0}$ and $u_z^{(k),0}$ are components of the displacement vector, $D_r^{(k),0}$ and $D_z^{(k),0}$ are the components of the electrical displacement vector, $E_r^{(k),0}$ and $E_z^{(k),0}$ are the components of the electric field vector, and $c_{ij}^{(k)}$, $e_{ij}^{(k)}$ and $\varepsilon_{nj}^{(k)}$ are the elastic, piezoelectric and dielectric constants, respectively.

In the case where the aforementioned ‘‘short-circuit’’ conditions are satisfied, the pre-critical state is determined according to the following expressions.

$$\begin{aligned}
\phi^{(k),0} &= 0, E_r^{(k),0} = E_z^{(k),0} = 0, \sigma_{zz}^{(k),0} = \sigma_{rz}^{(k),0} = 0, \sigma_{rr}^{(k),0} = \sigma_{\theta\theta}^{(k),0}, \\
s_{rr}^{(k),0} = s_{\theta\theta}^{(k),0} &= (c_{11}^{(k)} + c_{12}^{(k)})^{-1} \sigma_{rr}^{(k),0}, \sigma_{rr}^{(2),0} = \sigma_{rr}^{(1),0} (c_{11}^{(1)} + c_{12}^{(1)})^{-1} (c_{11}^{(2)} + c_{12}^{(2)}), \\
\sigma_{rr}^{(1),0} &= p \left(2 \frac{h_F}{h} + \frac{h_C}{h} \frac{(c_{11}^{(2)} + c_{12}^{(2)})}{(c_{11}^{(1)} + c_{12}^{(1)})} \right)^{-1}, \\
D_r^{(k),0} &= \left(e_{11}^{(k)} + e_{12}^{(k)} - \frac{c_{31}^{(k)} + c_{32}^{(k)}}{c_{33}^{(k)}} e_{13}^{(k)} \right) s_{rr}^{(k),0}, \\
D_z^{(k),0} &= \left(e_{31}^{(k)} + e_{32}^{(k)} - \frac{c_{31}^{(k)} + c_{32}^{(k)}}{c_{33}^{(k)}} e_{33}^{(k)} \right) s_{rr}^{(k),0}. \tag{2.2}
\end{aligned}$$

Note that the expressions in (2.1) and (2.2) are approximate in the near vicinity of the lateral boundary surface on which the external compressional radial forces act. Nevertheless, as we will consider the cases where $h/\ell \sim 10^{-1}$ (where $h = 2h_F + h_C$ (Fig. 1), therefore the influence of the mentioned proximity on the values of the critical parameters can be taken as insignificant one. Moreover, note that the expressions in (2.1) are obtained within the scope of the ‘‘open-circuit’’ condition satisfied on the face layers upper and lower plane-boundaries, according to which, the normal component of the electrical displacement vector on these planes is equal to zero.

Thus, within the scope of the foregoing assumptions, according to [5], [11], [2] the 3D linearized stability loss equations and relations for the case under consideration are obtained as follows:

3D linearized stability loss equations

$$\begin{aligned}
\frac{\partial t_{rr}^{(k)}}{\partial r} + \frac{\partial t_{zr}^{(k)}}{\partial z} + \frac{1}{r} (t_{rr}^{(k)} - t_{\theta\theta}^{(k)}) &= 0, \frac{\partial t_{rz}^{(k)}}{\partial r} + \frac{\partial t_{zz}^{(k)}}{\partial z} + \frac{1}{r} t_{rz}^{(k)} = 0, \\
\frac{\partial D_R^{(k)}}{\partial r} + \frac{1}{r} D_R^{(k)} + \frac{\partial D_Z^{(k)}}{\partial z} &= 0. \\
t_{rr}^{(k)} = \sigma_{rr}^{(k)} + \sigma_{rr}^{(k),0} \frac{\partial u_r^{(k)}}{\partial r} + M_{rr}^{(k)}, t_{\theta\theta}^{(k)} = \sigma_{\theta\theta}^{(k)} + \sigma_{\theta\theta}^{(k),0} \frac{u_r^{(k)}}{r} + M_{\theta\theta}^{(k)}, \\
t_{zr}^{(k)} = \sigma_{zr}^{(k)} + M_{zr}^{(k)}, t_{rz}^{(k)} = \sigma_{rz}^{(k)} + \sigma_{rr}^{(k),0} \frac{\partial u_z^{(k)}}{\partial r} + M_{rz}^{(k)}, t_{zz}^{(k)} = \sigma_{zz}^{(k)} + M_{zz}^{(k)}, \\
M_{rr}^{(k)} = E_r^{(k),0} E_r^{(k)} - E_\theta^{(k),0} E_\theta^{(k)} - E_z^{(k),0} E_z^{(k)}, \\
M_{\theta\theta}^{(k)} = E_\theta^{(k),0} E_\theta^{(k)} - E_r^{(k),0} E_r^{(k)} - E_z^{(k),0} E_z^{(k)}, \\
M_{zz}^{(k)} = E_z^{(k),0} E_z^{(k)} - E_\theta^{(k),0} E_\theta^{(k)} - E_r^{(k),0} E_r^{(k)}. \tag{2.3}
\end{aligned}$$

Linearized strain-displacement relations

$$s_{rr}^{(k)} = \frac{\partial u_r^{(k)}}{\partial r}, s_{\theta\theta}^{(k)} = \frac{u_r^{(k)}}{r}, s_{zz}^{(k)} = \frac{\partial u_z^{(k)}}{\partial z}, s_{rz}^{(k)} = \frac{1}{2} \left(\frac{\partial u_r^{(k)}}{\partial z} + \frac{\partial u_z^{(k)}}{\partial r} \right), \quad (2.4)$$

Linearized electro-mechanical relations

$$\begin{aligned} \sigma_{rr}^{(k)} &= c_{11}^{(k)} s_{rr}^{(k)} + c_{12}^{(k)} s_{\theta\theta}^{(k)} + c_{13}^{(k)} s_{zz}^{(k)} - e_{11}^{(k)} E_r^{(k)} - e_{31}^{(k)} E_z^{(k)}, \\ \sigma_{\theta\theta}^{(k)} &= c_{12}^{(k)} s_{rr}^{(k)} + c_{22}^{(k)} s_{\theta\theta}^{(k)} + c_{23}^{(k)} s_{zz}^{(k)} - e_{12}^{(k)} E_r^{(k)} - e_{32}^{(k)} E_z^{(k)}, \\ \sigma_{zz}^{(k)} &= c_{31}^{(k)} s_{rr}^{(k)} + c_{32}^{(k)} s_{\theta\theta}^{(k)} + c_{33}^{(k)} s_{zz}^{(k)} - e_{13}^{(k)} E_r^{(k)} - e_{33}^{(k)} E_z^{(k)}, \\ \sigma_{rz}^{(k)} &= c_{15}^{(k)} s_{rz}^{(k)} - e_{15}^{(k)} E_r^{(k)} - e_{35}^{(k)} E_z^{(k)}, \\ D_r^{(k)} &= e_{11}^{(k)} s_{rr}^{(k)} + e_{12}^{(k)} s_{\theta\theta}^{(k)} + e_{13}^{(k)} s_{zz}^{(k)} + \varepsilon_{11}^{(k)} E_r^{(k)} + \varepsilon_{13}^{(k)} E_z^{(k)}, \\ D_z^{(k)} &= e_{31}^{(k)} s_{rr}^{(k)} + e_{32}^{(k)} s_{\theta\theta}^{(k)} + e_{33}^{(k)} s_{zz}^{(k)} + \varepsilon_{31}^{(k)} E_r^{(k)} + \varepsilon_{33}^{(k)} E_z^{(k)}, \\ E_r^{(k)} &= -\frac{\partial \phi^{(k)}}{\partial r}, E_z^{(k)} = -\frac{\partial \phi^{(k)}}{\partial z}. \end{aligned} \quad (2.5)$$

Note that the relations in (2.1) - (2.3) are written for the piezoelectric materials and supposing that $e_{ij}^{(k)} = 0$ and $\varepsilon_{ij}^{(k)} = 0$ we can obtain the mechanical relations for the elastic materials. Moreover, note that under writing of the relations in (2.5) it is assumed that the polled direction of the piezoelectric material is the Oz axis direction (Fig. 1). At the same time, we assume that the contact and boundary conditions given below satisfy.

$$\begin{aligned} t_{zz}^{(3)} \Big|_{z=h_F+h_C} &= t_{zz}^{(2)} \Big|_{z=h_F+h_C}, t_{zr}^{(3)} \Big|_{z=h_F+h_C} = t_{zr}^{(2)} \Big|_{z=h_F+h_C}, \\ u_z^{(3)} \Big|_{z=h_F+h_C} &= u_z^{(2)} \Big|_{z=h_F+h_C}, \\ u_r^{(3)} \Big|_{z=h_F+h_C} &= u_r^{(2)} \Big|_{z=h_F+h_C}, t_{zz}^{(2)} \Big|_{z=h_F} = t_{zz}^{(1)} \Big|_{z=h_F}, t_{zr}^{(2)} \Big|_{z=h_F} = t_{zr}^{(1)} \Big|_{z=h_F}, \\ u_z^{(2)} \Big|_{z=h_F} &= u_z^{(1)} \Big|_{z=h_F}, u_r^{(2)} \Big|_{z=h_F} = u_r^{(1)} \Big|_{z=h_F}, \\ t_{zz}^3 \Big|_{z=2h_F+h_C} &= 0, t_{zr}^3 \Big|_{z=2h_F+h_C} = 0, t_{zz}^3 \Big|_{z=0} = 0, t_{zr}^1 \Big|_{z=0} = 0 \text{ for } 0 \leq r \leq l/2, \\ t_{rr}^{(k)} \Big|_{r=l/2} &= 0, u_z^{(k)} \Big|_{r=l/2} = 0, \text{ for } k = 1, 2, 3 \text{ under } r = l/2 \leq z \leq 2h_F + h_C. \end{aligned} \quad (2.6)$$

Note that the conditions given in (2.6) relate to the mechanical quantities and the corresponding conditions for the electrical quantities are given for the components of the electrical displacements $D_z^{(k)}$ and $D_r^{(k)}$, or for the electric potential $\phi^{(k)}$. In the case where we assume that the ‘‘open-circuit’’ conditions satisfy the following relations take place

$$D_z^{(3)} \Big|_{z=2h_F+h_C} = 0, D_z^{(3)} \Big|_{z=h_F+h_C} = 0, D_z^{(1)} \Big|_{z=0} = 0, D_z^{(1)} \Big|_{z=h_F} = 0, \quad (2.7)$$

$$\phi^{(3)} \Big|_{r=l/2} = 0, \phi^{(1)} \Big|_{r=l/2} = 0. \quad (2.8)$$

However in the case where we assume that the "short-circuit" conditions satisfy the relations in (2.7) are replaced with the following ones.

$$\phi^{(3)} \Big|_{z=2h_F+h_C} = 0, \phi^{(3)} \Big|_{z=h_F+h_C} = 0, \phi^{(1)} \Big|_{z=0} = 0, \phi^{(1)} \Big|_{z=h_F} = 0. \quad (2.9)$$

Consequently, in the present investigation we consider simultaneously two cases determined by conditions in (2.7) and (2.9).

This completes the formulation of the problem, according to which, the determination of the critical values of the pre-critical quantities is reduced to the solution of the eigenvalue problem (2.1), (2.3) – (2.8) for the "open-circuit" case, and (2.2),(2.3) – (2.6), (2.8) and (2.9) for the "short-circuit" case.

3 FEM modelling of the problem

We attempt to solve to the problem formulated in the previous section by employing FEM and for this purpose, according to [5], [11], [2] and others, we introduce the following functional.

$$\begin{aligned} \Pi(u_r^{(1)}, u_r^{(2)}, u_r^{(3)}, u_z^{(1)}, u_z^{(2)}, u_z^{(3)}, \phi^{(1)}, \phi^{(2)}, \phi^{(3)}) = \\ \frac{1}{2} \sum_{k=1}^3 \iint_{\Omega^{(k)}} \left[t_{rr}^{(k)} \frac{\partial u_r^{(k)}}{\partial r} + t_{\theta\theta}^{(k)} \frac{u_r^{(k)}}{r} + t_{rz}^{(k)} \frac{\partial u_z^{(k)}}{\partial r} + t_{zr}^{(k)} \frac{\partial u_r^{(k)}}{\partial z} + \right. \\ \left. + t_{zz}^{(k)} \frac{\partial u_z^{(k)}}{\partial z} + E_r^{(k)} D_r^{(k)} + E_z^{(k)} D_z^{(k)} \right] r dr dz, \end{aligned} \quad (3.1)$$

where

$$\begin{aligned} \Omega^{(1)} &= \{ 0 \leq r \leq l/2; 0 \leq z \leq h_F \}, \\ \Omega^{(2)} &= \{ 0 \leq r \leq l/2; h_F \leq z \leq h_F + h_C \}, \\ \Omega^{(3)} &= \{ 0 \leq r \leq l/2; h_F + h_C \leq z \leq 2h_F + h_C \}. \end{aligned} \quad (3.2)$$

From equating to zero the first variation of the functional (2.7), i.e. from the relation

$$\delta \Pi = \sum_{k=1}^3 \frac{\partial \Pi}{\partial u_r^{(k)}} \delta u_r^{(k)} + \sum_{k=1}^3 \frac{\partial \Pi}{\partial u_z^{(k)}} \delta u_z^{(k)} + \sum_{k=1}^3 \frac{\partial \Pi}{\partial \phi^{(k)}} \delta \phi^{(k)} = 0, \quad (3.3)$$

and after well-known mathematical manipulations we obtain the first three equations in (2.3). The boundary and contact conditions in (2.6) and (2.7) are given with respect to the forces and electrical displacements. In this way it is proven that the first three equations in (2.3) are the Euler equations for the functional (3.1) and the boundary and contact conditions in (2.6) and (2.7) which are given with respect to the forces and electrical displacements, are the related natural boundary and contact conditions.

According to FEM modelling, the solution domains indicated in (3.2) are divided into a finite number of finite elements. For the considered problem each of the finite elements is selected as a standard rectangular Lagrange family quadratic finite element (i.e. with nine nodes) and each node has three degrees of freedom, i.e. radial displacement $u_r^{(k)}$, transverse

displacement $u_z^{(k)}$ and electric potential $\phi^{(k)}$. Employing the standard Ritz technique detailed in many references, for instance, in the book by [13], we determine the displacements and electrical potential at the selected nodes. After this determination, from the equation

$$\det(K) = 0 \quad (3.4)$$

the values of the critical compressional forces are determined, where K is a corresponding stiffness matrix. The solution procedure of the equation (3.4) is made according to the well-know ‘‘bi-section’’ method which basis on the sign change of the $\det(K)$.

Note that in the ‘‘open-circuit’’ case under FEM modeling the nodes on the planes $z = 0$, h_F , $h_F + h_C$ and $2h_F + h_C$ the electrical potentials $\phi^{(1)}$ and $\phi^{(3)}$ are taken as unknown ones, however in the ‘‘short-circuit’’ case these potentials are taken as known ones and are equated to zero. Namely with these the FEM modeling in the ‘‘short-circuit’’ case is distinguished with that in the ‘‘open-circuit’’ case.

This completes the consideration of the method of solution.

4 Numerical results and discussions

Note that in the present paper, the piezoelectric materials PZT -5H, PZT -4 and BaTiO3 are taken as the face layer materials, however the metal materials - aluminum (Al) and steel (St) are taken as the core layer materials. The values of the elastic, piezoelectric and dielectric constants of the selected piezoelectric materials and the references used are given in Table 1.

Table 1. The values of the mechanical, piezoelectrical and dielectrical constants of the selected piezoelectric materials

Materials (Source Ref)	$c_{11}^{(r1)}$	$c_{12}^{(r1)}$	$c_{13}^{(r1)}$	$c_{33}^{(r1)}$	$c_{44}^{(r1)}$	$c_{66}^{(r1)}$	$e_{31}^{(r1)}$	$e_{33}^{(r1)}$	$e_{15}^{(r1)}$	$\varepsilon_{11}^{(r1)}$	$\varepsilon_{33}^{(r1)}$
PZT-4 [11]	13.9	7.78	7.40	11.5	2.56	3.06	-5.2	15.1	12.7	0.646	.562
PZT-5H [11]	12.6	7.91	8.39	11.7	2.30	2.35	-6.5	23.3	17.0	1.505	1.302
BaTiO3 [8]	16.6	7.66	7.75	16.2	4.29	4.29	-4.4	18.6	11.6	1.434	1.182
	$\times 10^{10} N/m^2$						C/m^2			$\times 10^{10} C/Vm$	

Table 2. The values of the critical dimensionless stresses σ_{cr}^1 , σ_{cr}^2 and \bar{p}_{cr} obtained for the case where the material of the core layer is Steel in the cases where the piezoelectric constants of PZT are equated to zero (upper number), the ‘‘short-circuit’’ (middle number) and the ‘‘open-circuit’’ conditions (lower number) satisfy and the piezoelectric and dielectric constants are equal to the corresponding data given in Table 1

h_F/l	Crit. Param.	Materials of the face layers		
		PZT-5H	PZT-4	BaTiO ₃
1/40	$\sigma_{cr}^{(2.1)}$	0.1015	0.1399	0.1249
		0.1017	0.1401	0.1249
		0.1925	0.2244	0.1418
$\sigma_{cr}^{(2.2)}$	$\sigma_{cr}^{(2.2)}$	0.3246	0.3120	0.2010
		0.3251	0.3123	0.2010
		0.3578	0.3375	0.2053
\bar{p}_{cr}	\bar{p}_{cr}	0.2689	0.2690	0.1820
		0.2693	0.2693	0.1820
		0.3165	0.3093	0.1895
1/30	$\sigma_{cr}^{(2.1)}$	0.0946	0.1337	0.1222
		0.0950	0.1342	0.1222
		0.1858	0.2194	0.1394
$\sigma_{cr}^{(2.2)}$	$\sigma_{cr}^{(2.2)}$	0.3026	0.2982	0.1965
		0.3037	0.2991	0.1967
		0.3453	0.3302	0.2019
\bar{p}_{cr}	\bar{p}_{cr}	0.2333	0.2434	0.1718
		0.2342	0.2442	0.1719
		0.2922	0.2933	0.1811
1/24	σ_{cr}^1	0.0896	0.1296	0.1206
		0.0904	0.1304	0.1208
		0.1816	0.2165	0.1381
$\sigma_{cr}^{(2.2)}$	$\sigma_{cr}^{(2.2)}$	0.2866	0.2888	0.1940
		0.2890	0.2908	0.1944
		0.3377	0.3258	0.2000
\bar{p}_{cr}	\bar{p}_{cr}	0.2046	0.2225	0.1635
		0.2063	0.2240	0.1638
		0.2727	0.2803	0.1743
1/20	σ_{cr}^1	0.0887	0.1274	0.1202
		0.0881	0.1290	0.1206
		0.1800	0.2156	0.1379
σ_{cr}^2	σ_{cr}^2	0.2774	0.2841	0.1933
		0.2818	0.2875	0.1939
		0.3345	0.3243	0.1998
\bar{p}_{cr}	\bar{p}_{cr}	0.1821	0.2058	0.1568
		0.1850	0.2083	0.1573
		0.2573	0.2700	0.1689

According to [6], the values of Lamé's constants of the core layer material is selected as follows: for the Al: $\lambda = 48.1 \text{ GPa}$ and $\mu = 27.1 \text{ GPa}$; for the St: $\lambda = 92.6 \text{ GPa}$ and $\mu = 77.5 \text{ GPa}$.

Under FEM modelling using the symmetry with respect to the plane $z = h_F + h_C/2$ and the axial symmetry with respect to the Oz (Fig. 1a) axis of the mechanical and geometrical properties of the plate, we consider only the region $\{0 \leq r \leq \ell/2; 0 \leq z \leq h_F + h_C\}$ and this region is divided into 40 finite elements along the radial direction and 12 finite elements along the plate's thickness direction, resulting in 31022 NDOF. Such selection of the finite elements numbers is established according to the convergence of the numerical results. All the corresponding PC programs are composed by the authors of the paper.

The algorithm and programs employed in the present investigations are some modifications and development of the corresponding algorithm and programs used and testing in the many investigations and discussed in the monograph by [1]. Consequently, the validity and trustiness of the used in the present investigations PC programs and algorithm cause no doubt.

For simplification of the consideration, we introduce the following notation for the dimensionless critical radial stresses and critical compressive forces:

$$\sigma_{cr}^{(1)} = \sigma_{rr.cr}^{(1),0} / c_{44}^{(1)}, \sigma_{cr}^{(2)} = \sigma_{rr.cr}^{(2),0} / c_{44}^{(1)}, \bar{p}_{cr} = p / c_{44}^{(1)}. \quad (4.1)$$

Thus, according to (4.1), we estimate the work carrying capacity of the plate under consideration with respect to the stability loss by simultaneous use of the values of three dimensionless critical parameters which are the dimensionless radial compressive stress $\sigma_{cr}^{(1)}$ in the face piezoelectric layer, the dimensionless radial compressive stress $\sigma_{cr}^{(2)}$ in the core metal layer and the dimensionless intensity \bar{p}_{cr} of the external compressive force. Such an approach for estimation of the buckling delamination allows us to have more precise information on the influence of the problem parameters such as the piezoelectricity of the face layers' materials, the face layers' thickness and the mechanical properties of the layers' materials.

Thus, we consider the numerical results obtained for the critical parameters indicated in (4.1) and detailed above. Note that these results are given in Tables 2 and 3 which are obtained for the cases where the material of the core layer is St and Al respectively. Moreover, note that these results are obtained for the cases where face layers materials are PZT-5H, PZT-4 and $BaTiO_3$. For estimation of the influence of the face layers' piezoelectricity on the values of the critical stresses in the tables, three types of results are presented simultaneously, the first of which (upper number) relates to the case where the values of the piezoelectric and dielectric constants of the face layer materials are equated to zero, i.e. coupling of the mechanical and electrical fields is not taken into consideration. However, under obtaining the second (third type) of results indicated by the middle numbers (by the lower numbers) the values of the piezoelectric and dielectric constants are taken into consideration as given in Table 1 and the coupling effect between the electrical and mechanical fields is taken into consideration completely and the "short-circuit" (2.9) (the "open-circuit" (7)) condition is satisfied.

Analysis of the results shows that for all the cases under consideration the piezoelectricity of the face layers causes an increase in the values of the dimensionless critical stresses σ_{cr}^1 , σ_{cr}^2 , and \bar{p}_{cr} . However this increase is more significant for the PZT-5H and PZT-4 than that for the $BaTiO_3$. At the same time, this increase is very significant for the "open-circuit" case than that for the "short-circuit" case.

Table 3. The values of the critical dimensionless stresses σ_{cr}^1 , σ_{cr}^2 and \bar{p}_{cr} obtained for the case where the material of the core layer is Aluminum in the cases where the piezoelectric constants of PZT are equated to zero (upper number), the "short-circuit" (middle number) and the "open-circuit" conditions (lower number) satisfy and the piezoelectric and dielectric constants are equal to the corresponding data given in Table 1

h_F/l	Crit. Param.	Materials of the face layers		
		PZT-5H	PZT-4	$BaTiO_3$
1/40	$\sigma_{cr}^{(1)}$	0.1264	0.1772	0.1586
		0.1268	0.1776	0.1587
		0.2430	0.2828	0.1793
$\sigma_{cr}^{(2)}$	$\sigma_{cr}^{(2)}$	0.1491	0.1458	0.0941
		0.1495	0.1461	0.0942
		0.1667	0.1570	0.0958
\bar{p}_{cr}	\bar{p}_{cr}	0.1435	0.1537	0.1103
		0.1439	0.1540	0.1104
		0.1858	0.1884	0.1167
1/30	$\sigma_{cr}^{(1)}$	0.1259	0.1777	0.1590
		0.1267	0.1786	0.1593
		0.2434	0.2823	0.1792
$\sigma_{cr}^{(2)}$	$\sigma_{cr}^{(2)}$	0.1485	0.1461	0.0944
		0.1494	0.1469	0.0946
		0.1670	0.1567	0.0957
\bar{p}_{cr}	\bar{p}_{cr}	0.1410	0.1567	0.1160
		0.1419	0.1575	0.1162
		0.1925	0.1986	0.1236
1/24	$\sigma_{cr}^{(2.1)}$	0.1259	0.1773	0.1580
		0.1274	0.1790	0.1584
		0.2422	0.2795	0.1775
$\sigma_{cr}^{(2.2)}$	$\sigma_{cr}^{(2.2)}$	0.1485	0.1458	0.0938
		0.1503	0.1472	0.0940
		0.1662	0.1552	0.0948
\bar{p}_{cr}	\bar{p}_{cr}	0.1391	0.1590	0.1206
		0.1408	0.1605	0.1209
		0.1979	0.2070	0.1293
1/25	σ_{cr}^1	0.1261	0.1762	0.1559
		0.1288	0.1791	0.1567
		0.2402	0.2750	0.1746
σ_{cr}^2	σ_{cr}^2	0.1488	0.1449	0.0926
		0.1519	0.1474	0.0930
		0.1647	0.1527	0.0933
\bar{p}_{cr}	\bar{p}_{cr}	0.1375	0.1606	0.1243
		0.1404	0.1633	0.1249
		0.2205	0.2139	0.1340

The discussed above character of the influence of the piezoelectricity of the face layers materials on the values of the dimensionless critical stresses can be explained with the so-called "piezoelectric stiffening" effect of the piezoelectric materials, i.e. with the increase of the material stiffness as a result of the piezoelectricity of that. The mentioned "piezoelectric stiffening" effect in the "open-circuit" case is more significant than that in the "short-circuit" case.

Consequently, the fact that an increase of the thickness of the face layers also increases the stiffness of the piezoelectric layers. However, under fixed h/l ($=0.2$) thickness of the plate an increase h_F/l causes a decrease of the h_C/l as a result of which the whole stiffness of the plate depends on the ratio of stiffnesses of the core and face layers materials. Under explanation of the results discussed above it is also necessary to take into consideration of the complicate character of the dependence between the selected dimensionless critical stress and the ratio of the stiffnesses of the layers.

Namely with the foregoing statements it can be explained the character of the influence of the change h_F/l on the values of the critical stresses. According to the results given in Tables 2 and 3 this character can be formulated as follows:

- 1 For the pairs of materials consisting of PZT + St an increase in the values of h_F/l causes to decrease in all the values of the critical stresses under consideration;
- 2 For the pairs of materials consisting of PZT + Al the values of \bar{p}_{cr} increase with h_F/l , however dependence among σ_{cr}^1 , σ_{cr}^2 and h_F/l has non-monotonic character;
- 3 The foregoing conclusions take place not only in the “open-circuit” case but also in the “short-circuit” case.

This completes the discussions of the obtained numerical results.

5 Conclusions

Thus, in the present paper within the scope of 3D linearized theory of stability for piezoelectric materials, the axisymmetric stability loss of the PZT/Metal/PZT sandwich circular plate has been investigated. The cases where “open-circuit” and “short-circuit” conditions with respect to the electrical displacement and electric potential respectively on the upper and lower surfaces, and short-circuit conditions with respect to the electrical potential on the lateral surface of the face layers are satisfied, are considered. The corresponding eigenvalue problem is solved numerically by employing FEM. Numerical results are presented in Tables 2 and 3 for the PZT-5H/Al/PZT-5H, PZT-4/Al/PZT-4, BaTiO₃/Al/BaTiO₃, PZT-5H/St/PZT-5H, PZT-4/St/PZT-4 and BaTiO₃/St/ BaTiO₃ plates, respectively. These results illustrate simultaneously the values of the critical dimensionless radial compressive stress $\sigma_{cr}^{(1)}$ acting in the face piezoelectric layer, the values of the dimensionless critical compressive radial stress $\sigma_{cr}^{(2)}$ acting in the core-metal layer and the values of the dimensionless critical stress of the intensity \bar{p}_{cr} of the external compressive forces obtained in the case where the piezoelectricity, i.e. the coupling effect, are taken into consideration (middle and lower numbers in the tables) and in the case where the coupling effect is not taken into consideration (upper number in the tables). According to these results, the concrete conclusions on the influence of the electro-mechanical and geometrical parameters of the sandwich circular plate under consideration on the values of the dimensionless stresses are made. Note that these conclusions are formulated in the text of the previous section and the main of them is the increase of the critical stresses as a result of the piezoelectricity of the face layers materials and the great magnitude of this increase in the “open-circuit” case than that in the “short-circuit” case.

References

1. Akbarov, S.D.: Stability Loss and Buckling Delamination: Three-Dimensional Linearized Approach for Elastic and Viscoelastic Composites. *Springer, Heidelberg, New York* (2013).

2. Akbarov, S.D., Yahnioglu, N.: *Buckling delamination of a sandwich plate-strip with piezoelectric face and elastic core layers*, Appl. Math. Model. **37**, 8029 – 8038 (2013).
3. Akbarov, S.D., Rzayev, O.G.: *On the buckling of the elastic and viscoelastic composite circular thick plate with a penny-shaped crack*, Eur. J Mech. A Solid. **21** (2), 269 – 279 (2002).
4. Arefi, M., Allam, M.N.M.: *Nonlinear responses of an arbitrary FGP circular plate resting on the Winkler – Pasternak foundation*, Smart Structures and Systems, **16** (1), 81–100 (2015).
5. Guz, A.N.: *Fundamentals of the Three-Dimensional Theory of Stability of Deformable Bodies*. Springer-Verlag, Berlin Heidelberg (1999).
6. Guz, A.N.: *Elastic waves in bodies with initial (residual) stresses*. A.C.K., Kiev (2004).
7. Jabbari, M., Farzaneh, Joubaneh, E., Khorshidvand, A.R., Eslami, M.R.: *Buckling analysis of porous circular plate with piezoelectric actuator layers under uniform radial compression*, Int. J. Mech. Science. **70**: 50–56 (2013).
8. Kuna, M.: *Finite element analysis of cracks in piezoelectric structures: a survey*, Arch. Appl. Mech. **76**, 725–745 (2006).
9. Rzayev, O.G., Akbarov, S.D.: *Local buckling of the elastic and viscoelastic coating around the penny-shaped interface crack*, Int. J Eng. Sci. **40**, 1435–1451 (2002).
10. Wu, C.P., Ding, S.: *Coupled electro-elastic analysis of functionally graded piezoelectric material plates*, Smart Structures and Systems, **16** (5), 781–806 (2015).
11. Yang, J.S.: *Buckling of a piezoelectric plate*, Int. J. Appl. Electromagn. Mech, **9**, 399–408 (1998).
12. Yang, J.S.: *An introduction to the theory of piezoelectricity*. Springer, New-York (2005).
13. Zienkiewicz, O.C., Taylor, R.L.: *Basic formulation and linear problems. The finite element method*, **1**, 4-th edn. McGraw-Hill, New York (1989).